Influence of Geometric Nonlinearities in the Dynamics of Flexible Treelike Structures

S. K. Ider* and F. M. L. Amirouche†
University of Illinois at Chicago, Chicago, Illinois

A comprehensive computer algorithm used in the dynamic analysis of multibody systems is presented. The procedures developed combine Kane's equations, the strain energy, and modal analysis to describe the elastic bodies. The equations of motion are expressed in a form in which their coefficients are based on the partial velocity and partial angular velocity arrays and are easily coded for computers. The nonlinear geometric stiffness matrix is developed for three-dimensional beams that account for the couplings between the deformation components having significant effects in high-speed systems. The method presented in this paper is tailored for structures with variable cross-sectional beam elements such as spacecraft antennae, helicopter rotor blades, robot systems, and mechanisms. The effects of rotary inertia as well as shear deformation are automatically included into the equations of motion. A method for obtaining the shape function matrix consisting of assumed dynamic modes is also presented. In addition, the preceding formulations are used in a simulation of a space-based robotic manipulator, and the results are compared with those obtained by Kane et al. in Ref. 20.

I. Introduction

DYNAMIC analysis of multibody systems has gained tremendous popularity and attention by concerned dynamicists and researchers. Rigid and flexible bodies have been the subject of numerous publications and it would be rather poor judgment to only refer to few. In the last decade alone we have seen general-purpose programs written that claim they can solve a number of problems in rigid-body dynamics, including the effects of flexibility.[1–5] One of the burdens that these existing programs carry is in the application itself; in most cases the user has to make a number of changes to make the program suitable for the problem in question.

In robotics,[6–12] where the modeling of elastic deformation of links is based on beam analysis, certain terms due to the beam deformation are omitted to gain speed for off-line programming. Similar mistakes in aircraft dynamics[13–15] and mechanisms[16–19] are found where the rigid-body motion is assumed to be unaffected by the elastic deformations or the contributions due to the geometric couplings between the deformation components.

Recently it has been shown that the geometric nonlinearities arising from the coupling of longitudinal and transverse deformations have considerable effect on the deformation of beams in high-speed systems.[20] In Ref. 20 the effects of this coupling have been considered in the generalized inertia forces utilizing the proper constraint equations between the elastic coordinates. In this paper the geometric stiffening effects are accounted for in the formulation of the strain energy equations by extending the methods presented in Ref. 24 to three dimensions.

The computer-oriented procedure presented herein provides automatic generation of the equations of motion of flexible multibody systems in a general tree topology, taking into account the complete nonlinear interactions between the elastic deformations and the gross rigid-body motion.

A lumped-mass approach is formulated that has the advantage of ease of implementation and programming. This approach is modified by including the rotary inertia effects by making use of the average rotations of the grid elements. This is particularly important for beams in multibody systems undergoing large gross rotations and enables one to use a considerably smaller number of elements for accurate simulations. Furthermore, component mode techniques[26] are used to reduce the elastic coordinates.

An explicit formulation of the partial velocities and partial angular velocities in treelike flexible structures is also presented. It should be noted that only Huston and Passarello[22] have successfully formulated those arrays for rigid-body dynamics.

The equations presented herein add a new dimension to the study of mechanical structures with beam-type bodies. These beams could be of variable cross-sectional areas and material properties that vary from segment to segment.

The user-friendly built-in array called the "tree array" is used to describe the topology of the structure and serves as a basis for the kinematics and dynamics.

This paper consists of five sections. The first section describes the system configuration and geometry organization. In the second section a description of the modeling of a flexible body and detailed derivation of the kinematics are presented. The equations of motion derived via Kane's equations are given in Sec. III. In Sec. IV a simulation of a space robotic system is presented. The conclusion forms the last section.

II. System Description

The system is composed of rigid and flexible bodies forming a treelike structure as shown in Fig. 1. The bodies are interconnected by joints that have three rotational and three translational degrees of freedom.

The flexible bodies in the system are modeled by beams undergoing small deformations in all directions. The beam may have variable cross-sectional area along its length with the restriction that the principal axes at each cross-section are parallel. For simplicity the shear center is assumed to coincide with the centroidal axis. In the formulation of the equations of motion, all bodies will be considered flexible. The rigid bodies that may have arbitrary shapes are represented as special cases.

The topology of the structure will be described by means of a tree array $\Gamma^i(k)$ to keep track of the bodies with respect to one another as described below.

Let the number of the bodies in the structure be N. Arbitrarily select one of the bodies as reference body 1 (B_1),

Received May 18, 1988; revision received Aug. 22, 1988.

*Graduate Assistant. Member AIAA.
†Assistant Professor. Member AIAA.

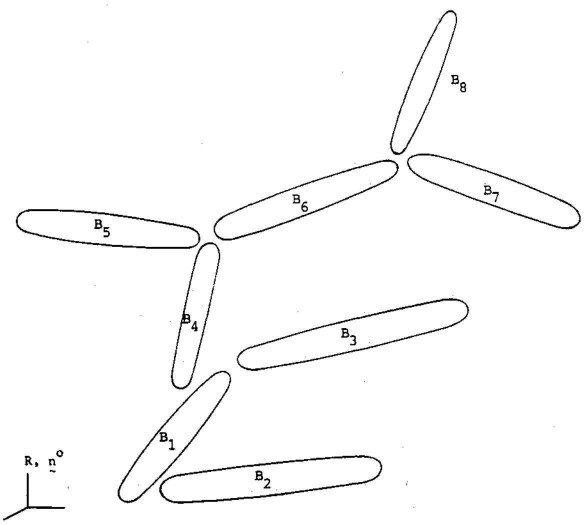

Fig. 1 A multibody structure.

and label the other bodies in the system in ascending progression away from B_1. Let the number 0 refer to a stationary reference frame R. Then let $\Gamma^0(k)$ denote k and $\Gamma^1(k)$ denote the adjacent lower body connected to B_k. Knowing $\Gamma^0(k)$ and $\Gamma^1(k)$ for $k = 1,..., N$, one can generate $\Gamma^i(k)$, $i > 2$. Finally, let $H(k)$ represent the maximum order h for which $\Gamma^h(k)$ is nonzero for B_k. Then the tree array $\Gamma^i(k)$, $i = 1,..., H(k)$ indicates the chain of bodies that are on the path from B_k to the reference frame. In the derivation of the equations for the kinematics, we will use the tree array as a basis for our analysis. (Further details on the tree array could be found in Ref. 23.)

In the notation, the summation sign is omitted in the equations such that a repeated subscript index in a term implies summation over the range of that index. Superscripts are generally part of the labeling and do not imply summation unless otherwise explicitly stated.

III. Kinematics of Flexible Bodies

1. Representation of a Flexible Body

In Fig. 2, two typical connecting bodies B_k and B_j where $j = \Gamma(k)$ are shown. The connection points assumed to lie on the centroidal line of the respective bodies are denoted by O_k and O_k^*, on B_k and B_j, respectively. The rigid-body degrees of freedom of B_k are characterized by the relative translation and rotation of the $\boldsymbol{n}^k$ axis fixed at O_k with respect to the $\boldsymbol{n}^{k*}$ axis (fixed at O_k^*). Let $\boldsymbol{n}^k$ be the body reference axis relative to which the deformation of the body will be defined. B_k will be considered to be composed of E_k number of small elements in the manner shown in Fig. 2, where $\boldsymbol{r}^{ki}$ is the undeformed vector from O_k to the mass center of ith element. Let $\boldsymbol{n}^{ki}$ represent the axis fixed in this element. Finally, let $\boldsymbol{n}^k$, $\boldsymbol{n}^{k*}$, and $\boldsymbol{n}^{ki}$ be oriented such that $\boldsymbol{n}_1^k$, $\boldsymbol{n}_1^{k*}$, and $\boldsymbol{n}_1^{ki}$ are tangent to the centroidal line and the second and third components form the principal axes of the cross section.

The local motion of the element due to deformation with respect to $\boldsymbol{n}^k$ can be described by three translation components u_1^{ki}, u_2^{ki}, and u_3^{ki} and three rotation components θ_1^{ki}, θ_2^{ki}, and θ_3^{ki} representing the rotation of $\boldsymbol{n}^{ki}$ with respect to $\boldsymbol{n}^k$.

To enable us to represent the deformation behavior of the body in terms of a small number of deformation coordinates, we will make use of the deformation-mode shapes. It is required that the mode shapes satisfy the geometric boundary conditions.

The deformation displacement and rotation u_p^{ki} and θ_p^{ki}, $p = 1,2,3$, can be expressed as

$$u_p^{ki} = \phi_{pr}^{ki}\eta_r^k, \qquad p = 1,2,3; \qquad r = 1,..., M_k \tag{1}$$

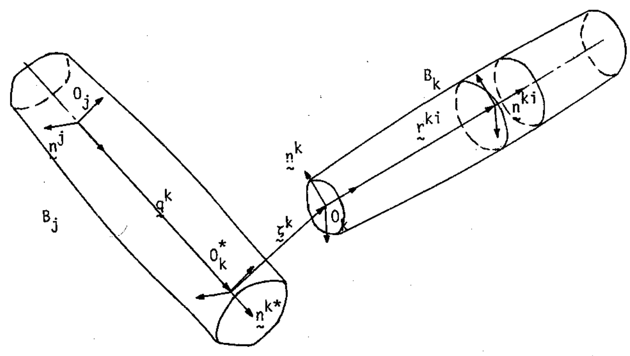

Fig. 2 Labeling position vectors in adjacent bodies.

and

$$\theta_p^{ki} = \psi_{pr}^{ki}\eta_r^k \tag{2}$$

where η_r^k, $r = 1,..., M_k$ are the modal coordinates of B_k and ϕ^{ki} and ψ^{ki} are the shape matrices in modal coordinates for the deformation displacement and rotation of the element mass center, respectively.

The shape function matrices ϕ^{ki} and ψ^{ki} can be determined by a finite-element numerical solution of the eigenvalue problem associated with the free vibration of the beam, as shown in Appendix A. They are obtained by making use of discrete-mode shapes of the eigenvalue problem together with the element shape functions.

Alternative to the numerical solution, one may wish to neglect the shear-deformation effects and determine u_p^{ki} and θ_p^{ki} for the selected grid points i, by utilizing the simple analytical eigenfunctions for the transverse, torsional, and longitudinal vibrations.

2. Generalized Coordinates

The relative angular velocity of $\boldsymbol{n}^k$ with respect to $\boldsymbol{n}^{k*}$ representing the relative rigid-body angular motion of B_k can be written as

$$^{\boldsymbol{n}^{k*}}\boldsymbol{\omega}^{\boldsymbol{n}^k} = \hat{\omega}_1^k\boldsymbol{n}_1^{k*} + \hat{\omega}_2^k\boldsymbol{n}_2^{k*} + \hat{\omega}_3^k\boldsymbol{n}_3^{k*} \tag{3}$$

where $\hat{\omega}_p^k$, $p = 1,2,3$ denote the relative angular velocity components.

The relative transformation vector $\boldsymbol{\zeta}^k$ is the relative translation of $\boldsymbol{n}^k$ with respect to $\boldsymbol{n}^{k*}$:

$$\boldsymbol{\zeta}^k = \zeta_1^k\boldsymbol{n}_1^{k*} + \zeta_2^k\boldsymbol{n}_2^{k*} + \zeta_3^k\boldsymbol{n}_3^{k*} \tag{4}$$

The relative translational velocity components denoted as $\dot{\zeta}_i^k$ are the components of the derivative of $\boldsymbol{\zeta}^k$ in the local axis $\boldsymbol{n}^{k*}$

$$^{\boldsymbol{n}^{k*}}\dot{\boldsymbol{\zeta}}^k = \dot{\zeta}_1^k\boldsymbol{n}_1^{k*} + \dot{\zeta}_2^k\boldsymbol{n}_2^{k*} + \dot{\zeta}_3^k\boldsymbol{n}_3^{k*} \tag{5}$$

The time derivatives of deformation translation and rotation components of B_k in the local axis $\boldsymbol{n}^k$ are, from Eqs. (1) and (2),

$$\dot{u}_p^{ki} = \phi_{pj}^{ki}\dot{\eta}_j^k; \qquad p = 1,2,3, \qquad j = 1,...,M_k \tag{6}$$

and

$$\dot{\theta}_p^{ki} = \psi_{pj}^{ki}\dot{\eta}_j^k, \qquad p = 1,2,3, \qquad j = 1,...,M_k \tag{7}$$

where $\dot{\eta}_j$ are the modal coordinate derivatives.

Let the generalized speeds of the system be defined as y_ℓ, $\ell = 1, \ldots, 6N + M$, where the first $3N$ represent the relative angular velocity components $\hat{\omega}_p$, the next $3N$ represent the relative translational velocity components $\dot{\zeta}_p$, and the last M

represent the modal coordinate derivatives $\dot{\eta}_p$. These are expressed as

$$\hat{\omega} = [\hat{\omega}_1^1, \hat{\omega}_2^1, \hat{\omega}_3^1, \ldots, \hat{\omega}_1^k \hat{\omega}_2^k, \hat{\omega}_3^k, \ldots, \hat{\omega}_1^N, \hat{\omega}_2^N, \hat{\omega}_3^N]^T \quad (8)$$

$$\zeta = [\zeta_1^1, \zeta_2^1, \zeta_3^1, \ldots, \zeta_1^k, \zeta_2^k, \zeta_3^k, \ldots, \zeta_1^N, \zeta_2^N, \zeta_3^N]^T \quad (9)$$

$$\dot{\eta} = [\dot{\eta}_1^1, \ldots, \dot{\eta}_{M_1}^1, \ldots, \dot{\eta}_1^k, \ldots, \dot{\eta}_{M_k}^k, \ldots, \dot{\eta}_1^N, \ldots, \dot{\eta}_{M_N}^N]^T \quad (10)$$

$$y = [\hat{\omega}^T, \zeta^T, \dot{\eta}^T]^T \quad (11)$$

There is more than one way to describe the relative angular orientations for the axis systems. This includes orientation angles and Euler parameters. In this paper the relative angular orientations of the body reference axis are described by transformation matrices that can be expressed in terms of relative orientation angles or Euler parameters.

Therefore, it is convenient to describe the geometry and the kinematics of the system with the generalized speeds described previously together with $3N$ relative translation components, M modal coordinates, and $3N$ relative orientation angles or $4N$ Euler parameters.

3. Angular Velocities

Let S^{0k} denote the transformation matrix between $\boldsymbol{n}^k$ and $\boldsymbol{n}^0$, and S^{0k*} denote the transformation matrix between $\boldsymbol{n}^{k*}$ and $\boldsymbol{n}^0$.

The time derivative of S^{0k}, which will be needed in the analysis, can be obtained as shown in Ref. 22:

$$\frac{dS_{ij}^{0k}}{dt} = -\omega_n^k e_{imn} S_{mj}^{0k}, \qquad i,j,m,n = 1,2,3 \quad (12)$$

where ω_n^k are the components of the angular velocity $\boldsymbol{\omega}^k$ of $\boldsymbol{n}^k$ in R, and e_{imn} is the standard permutation symbol.

The angular velocity of the element i in B_k with respect to the inertial frame R can be expressed as the sum of relative angular velocities:

$$\boldsymbol{\omega}^{ki} = {}^{n^0-n^1}\boldsymbol{\omega} + {}^{n^1-n^{2*}}\boldsymbol{\omega} + {}^{n^{2*}-n^2}\boldsymbol{\omega} + \cdots + {}^{n^j-n^{k*}}\boldsymbol{\omega} + {}^{n^{k*}-n^k}\boldsymbol{\omega} + {}^{n^k-n^{ki}}\boldsymbol{\omega} \quad (13)$$

where ${}^{n^{k*}-n^k}\boldsymbol{\omega}$ is defined by Eq. (3).

The ${}^{n^j-n^{k*}}\boldsymbol{\omega}$ is the relative angular velocity of $\boldsymbol{n}^{k*}$ with respect to $\boldsymbol{n}^j$ due to the deformation of B_j. Utilizing Eq. (A10) in Appendix A, and assuming small rotations due to deformation, it can be expressed as

$${}^{n^j-n^{k*}}\boldsymbol{\omega} = \psi_{\ell p}^{k*}\dot{\eta}_p^j \boldsymbol{n}_\ell^j; \qquad \ell = 1,2,3, \qquad p = 1,\ldots, M_j \quad (14)$$

Similarly, from Eq. (7) the angular velocity of the element i relative to $\boldsymbol{n}^k$ can be written as

$${}^{n^k-n^{ki}}\boldsymbol{\omega} = \psi_{\ell p}^{ki}\dot{\eta}_p^k \boldsymbol{n}_\ell^k; \qquad \ell = 1,2,3, \qquad p = 1,\ldots, M_k \quad (15)$$

Substituting Eqs. (3), (14), and (15) into Eq. (13) and making use of the transformation matrices and the tree array $\Gamma^p(k)$, $p = 1,\ldots, H(k)$, we obtain

$$\boldsymbol{\omega}^{ki} = \left(\sum_{p=0}^{H} \hat{\omega}_u^s S_{mu}^{0s*} + \sum_{p=0}^{H} S_{mu}^{0r}\psi_{ut}^{r*}\dot{\eta}_t^r + S_{mu}^{0k}\psi_{ut}^{ki}\dot{\eta}_t^k \right)\boldsymbol{n}_m^0$$

$$m = 1,2,3, \qquad t = 1,\ldots, z_t \text{ or } M_k \quad (16)$$

where $s = \Gamma^p(k)$, $r = \Gamma(s)$.

Equation (16) is linear in the relative angular velocity components and modal coordinate derivatives. Therefore, it is convenient to write Eq. (16) by separating the coefficients of the generalized speeds:

$$\boldsymbol{\omega}^{ki} = (v_{\ell m}^k \hat{\omega}_\ell + \mu_{pm}^{ki}\dot{\eta}_p)\boldsymbol{n}_m^0, \quad \ell = 1,\ldots,3N; \quad p = 1,\ldots,M \quad (17)$$

where

$$v_{\ell m}^k = \sum_{h=0}^{H} S_{mu}^{0s*}B_{u\ell}^s, \qquad s = \Gamma^h(k) \quad (18)$$

and

$$\mu_{pm}^{ki} = \sum_{h=0}^{H} S_{mu}^{0r}\psi_{ut}^{r*}C_{tp}^r + S_{mu}^{0k}\psi_{mu}^{ki}C_{tp}^k, \qquad r = \Gamma(s) \quad (19)$$

where $v_{\ell m}^k$ and μ_{pm}^{ki} are the partial angular velocity arrays associated with $\hat{\omega}_\ell$ and $\dot{\eta}_p$, respectively. In Eqs. (18) and (19), B^k and C^k are Boolean matrices used for describing the indices of $\hat{\omega}_r^k$ in $\hat{\omega}_r$ and $\dot{\eta}_r^k$ in $\dot{\eta}_r$, respectively, defined as $\hat{\omega}_r^k = B_{rs}^k\hat{\omega}_s$ and $\dot{\eta}_r^k = C_{rs}^k\dot{\eta}_s$.

In a more compact form, Eq. (17) can be written as

$$\boldsymbol{\omega}^{ki} = \omega_{\ell m}^{ki} y_\ell \boldsymbol{n}_m^0 \quad (20)$$

where

$$\omega_{\ell m}^{ki} = \begin{cases} v_{\ell m}^k & \ell \leqslant 3N \\ 0 & 3N < \ell \leqslant 6N \\ \mu_{\ell-6N,m}^{ki} & 6N < \ell \leqslant 6N + M \end{cases} \quad (21)$$

The partial angular velocity arrays are functions of displacements only and need to be generated for each element i in body k. Consider an element i in B_4 in Fig. 1. Let each body have c modal coordinates. The angular velocity of $\boldsymbol{n}^{4i}$ is

$$\boldsymbol{\omega}^{4i} = (\delta_{\ell m} y_\ell + S_{\ell m}^{03*} y_{\ell+6} + S_{\ell m}^{04*} y_{\ell+9} + S_{sm}^{01}\psi_{m\ell}^{1*} y_{\ell+36}$$

$$+ S_{sm}^{03}\psi_{m\ell}^{3*} y_{\ell+36+2c} + S_{sm}^{04}\psi_{m\ell}^{4i} y_{\ell+36+3c})\boldsymbol{n}_m^0 \quad (22)$$

In the subsequent analysis the angular velocity of $\boldsymbol{n}^k$ with respect to $\boldsymbol{n}^0$ and the angular velocity of $\boldsymbol{n}^{k*}$ with respect to $\boldsymbol{n}^0$, denoted as $\boldsymbol{\omega}^k$ and $\boldsymbol{\omega}^{k*}$, respectively, are also needed. The $\boldsymbol{\omega}^k$ can be obtained by subtracting ${}^{n^k-n^{ki}}\boldsymbol{\omega}$ from Eq. (13)

$$\boldsymbol{\omega}^k = (v_{\ell m}^k \hat{\omega}_\ell + \mu_{pm}^k \dot{\eta}_p)\boldsymbol{n}_m^0 \quad (23)$$

where μ_{pm}^k is obtained by setting the last term in Eq. (19) to zero. Similarly, $\boldsymbol{\omega}^{k*}$ can be obtained by subtracting ${}^{n^{k*}-n^k}\boldsymbol{\omega}$ from $\boldsymbol{\omega}^k$. This yields

$$\boldsymbol{\omega}^{k*} = (v_{\ell m}^r \hat{\omega}_\ell + \mu_{pm}^k \dot{\eta}_p)n_m^0, \qquad r = \Gamma(k) \quad (24)$$

4. Angular Accelerations

The angular acceleration of the ith element in B_k is found by differentiating Eq. (20); hence,

$$\boldsymbol{\alpha}^{ki} = (\omega_{\ell m}^{ki}\dot{y}_\ell + \dot{\omega}_{\ell m}^{ki} y_\ell)\boldsymbol{n}_m^0 \quad (25)$$

The $\dot{v}_{kipm}$ and $\dot{\mu}_{kipm}$ are obtained by replacing the transformation matrices in Eqs. (18) and (19), respectively, by their derivatives utilizing Eq. (12). Note that $\dot{v}_{\ell m}^k$ and $\dot{\mu}_{\ell m}^{ki}$ are functions of angular velocity components as well as displacements.

5. Mass Center Velocities and Accelerations

The position vector from the fixed reference axis $\boldsymbol{n}^0$ in R to the mass center of the ith element in B_k is given by (with the notation of Fig. 2)

$$\boldsymbol{P}_{ki} = \sum_s \boldsymbol{\zeta}^s + \sum_s \boldsymbol{d}^s + \boldsymbol{r}^{ki} + \boldsymbol{u}^{ki} \quad (26)$$

where the summations are carried for the bodies along the path from B_k to R and where $\boldsymbol{d}^1 = 0$.

By differentiation, the mass center velocity of the element is obtained as

$$\boldsymbol{v}^{ki} = \sum_{q=0}^{H(k)} \boldsymbol{\omega}^{s^*} \times \boldsymbol{\zeta}^s + \sum_{q=0}^{H(k)} {}^{n^{s^*}}\dot{\boldsymbol{\zeta}}^s + \sum_{q=0}^{H(k)} \boldsymbol{\omega}^p \times \boldsymbol{d}^s + \sum_{q=0}^{H(k)} {}^{n^p}\dot{\boldsymbol{d}}^s + \boldsymbol{\omega}^k \times (\boldsymbol{r}^{ki} \times \boldsymbol{u}^{ki}) + {}^{n^k}\dot{\boldsymbol{u}}^{ki} \tag{27}$$

where $s = \Gamma^q(k)$ and $p = \Gamma(s)$.

The $\boldsymbol{d}^s$ can be written as

$$\boldsymbol{d}^s = \boldsymbol{q}^s + \phi^p_{mt}\eta^p_t \boldsymbol{n}^p_m, \qquad p = \Gamma(s) \tag{28}$$

where $\boldsymbol{q}^s$ is the vector in the undeformed state. The local derivative of $\boldsymbol{d}^s$ is then

$${}^{n^p}\dot{\boldsymbol{d}}^s = \phi^{p^*}_{mt}\dot{\eta}^p_t \boldsymbol{n}^p_m, \qquad p = \Gamma(s) \tag{29}$$

The local derivative of the relative translation vector $\boldsymbol{\zeta}^s$ is given in Eq. (5). Note that

$$\sum_s {}^{n^{s^*}}\dot{\boldsymbol{\zeta}}^s = \sum_s \dot{\zeta}^s_t S^{0s^*}_{mt}\boldsymbol{n}^0_m = v^k_{\ell m}\dot{\zeta}_\ell \boldsymbol{n}^0_m$$

$$\ell = 1,...,3N, \qquad m,t = 1,2,3 \tag{30}$$

The local derivative of $\boldsymbol{u}^{ki}$ is obtained from Eq. (6). Note that $\boldsymbol{r}^{ki}$ is the undeformed local position vector to the mass center of the ith element. Substituting Eqs. (28–30), (23), (24), and (6) into Eq. (27) and making use of the transformation matrices, we obtain

$$\boldsymbol{v}^{ki} = (\alpha^{ki}_{\ell m}\hat{\omega}_\ell + v^k_{\ell m}\dot{\zeta}_\ell + \beta^{ki}_{pm}\dot{\eta}_p)\boldsymbol{n}^0_m$$

$$\ell = 1,...,3N; \quad p = 1,...,M$$

$$k = 1,...,N, \quad i = 1,...,M_k \tag{31}$$

where

$$\alpha^{ki}_{\ell m} = \sum_{h=0}^{H} [v^r_{t\ell}\zeta^s_q S^{0s^*}_{uq} e_{mtu} + S^{0r}_{uq} d^s_q v^r_{t\ell} e_{mtu}] + S^{0k}_{uq}(r^{ki}_q + u^{ki}_q)v^k_{t\ell}e_{mtu}$$

$$s = \Gamma^h(k); \quad r = \Gamma(s); \quad \ell = 1,...,3N;$$

$$m,t,u,q = 1,2,3 \tag{32}$$

and

$$\beta^{ki}_{pm} = \sum_{h=0}^{H} [S^{0s^*}_{uq}\zeta^s_q \mu^s_{tp} e_{mth} + S^{0r}_{uq} d^s_q \mu^r_{tp} e_{mtu} + S^{0r}_{mt}\phi^{s^*}_{tv} C^r_{vp}] + S^{0k}_{uq}(r^{ki}_q + u^{ki}_q)\mu^k_{tp}e_{mtu} + S^{0k}_{mt}\phi^{ki}_{tv}C^k_{vp},$$

$$p = 1,...,M \tag{33}$$

Equation (31) can be expressed as

$$\boldsymbol{v}^{ki} = v^{ki}_{\ell m} y_\ell \boldsymbol{n}^0_m, \qquad \ell = 1,...,6N + M \tag{34}$$

where

$$v^{ki}_{\ell m} = \begin{cases} \alpha^{ki}_{\ell m} & \ell \leqslant 3N \\ v^k_{\ell - 3N,m} & 3N < \ell \leqslant 6N \\ \beta^{ki}_{\ell - 6N,m} & 6N < \ell \leqslant 6N + M \end{cases} \tag{35}$$

Note that $v^{ki}_{\ell m}$ depends on displacements only.

By differentiating Eq. (34) we obtain the acceleration of the mass center of the ith element in body k as

$$\boldsymbol{a}^{ki} = (v^{ki}_{\ell m}\dot{y}_\ell + \dot{v}^{ki}_{\ell m} y_\ell)\boldsymbol{n}^0_m \tag{36}$$

IV. Equations of Motion

Kane's equations are given by

$$F^*_\ell + F_\ell - F^s_\ell = 0, \qquad \ell = 1,...,6N + M \tag{37}$$

where F^*_ℓ and F_ℓ are the generalized inertia and external forces, and F^s_ℓ are the generalized internal forces due to strain energy of the deformable bodies. Let the externally applied force field on element i of B_k be represented by a force $\boldsymbol{F}^{ki}$ passing through the mass center and by a moment $\boldsymbol{M}^{ki}$. Similarly, let the inertia force system of the element be represented by a force $\boldsymbol{F}^{*ki}$ passing through the mass center and by a moment M^{*ki}, such that

$$\boldsymbol{F}^{*ki} = -m^{ki}\boldsymbol{a}^{ki} \tag{38}$$

$$\boldsymbol{M}^{*ki} = -\boldsymbol{I}^{ki}\cdot\boldsymbol{\alpha}^{ki} - \boldsymbol{\omega}^{ki} \times (\boldsymbol{I}^{ki}\cdot\boldsymbol{\omega}^{ki}) \tag{39}$$

where m^{ki} is the mass of the ith element and $\boldsymbol{I}^{ki}$ is the inertia dyadic of the element relative to its mass center and expressed in terms of the $\boldsymbol{n}^0$ axis.

The F_ℓ and F^*_ℓ could be expressed as

$$F_\ell = \sum_{k=1}^{N}\sum_{i=1}^{E_k}\left(\frac{\partial \boldsymbol{v}^{ki}}{\partial y_\ell}\cdot \boldsymbol{F}^{ki} + \frac{\partial \boldsymbol{\omega}^{ki}}{\partial y_\ell}\cdot \boldsymbol{M}^{ki}\right) \tag{40}$$

and

$$F^*_\ell = \sum_{k=1}^{N}\sum_{i=1}^{E_k}\left(\frac{\partial \boldsymbol{v}^{ki}}{\partial y_\ell}\cdot \boldsymbol{F}^{*ki} + \frac{\partial \boldsymbol{\omega}^{ki}}{\partial y_\ell}\cdot \boldsymbol{M}^{*ki}\right) \tag{41}$$

The generalized stiffness forces will be formulated to include the geometric stiffening of the transverse deformations, which are important in high-speed systems. These are obtained by formulating the strain energy of the deformable bodies by nonlinear strain displacement relations and retaining the higher-order coupling terms, as shown in Appendix B. The generalized stiffness forces F^s_ℓ take the following form:

$$F^s_{\ell+6N} = (K_{\ell p} + G_{\ell p})\eta_p, \qquad p,\ell = 1,...,M \tag{42}$$

where

$$K = \mathrm{diag}[K^1,...,K^N], \qquad G = \mathrm{diag}[G^1_1,...,G^N] \tag{43}$$

and

$$K^k_{\ell p} = X^k_{\ell r}\bar{K}^k_{rs}X^k_{sp}, \qquad G^k_{\ell p} = X^k_{\ell r}\bar{G}^k_{rs}X_{sp} \tag{44}$$

where $\bar{K}^k_{rs}$ is the assembled structural stiffness matrix of B_k, $\bar{G}^k_{rs}$ is the assembled geometric stiffness matrix of B_k, and X^k is the modal matrix (Appendix A). The $\bar{G}^k_{rs}$ as derived in Appendix B depends on the deformations and needs to be updated.

Substituting Eqs. (38–41) into Eq. (37), we obtain the equations of motion in a computer form as

$$b_{\ell q}\dot{y}_q = f_\ell \tag{45}$$

where

$$b_{\ell q} = \sum_{k=1}^{N}\sum_{i=1}^{E_k}(m^{ki}v^{ki}_{\ell m}v^{ki}_{qm} + I^{ki}_{mn}\omega^{ki}_{\ell m}\omega^{ki}_{qn}) \tag{46}$$

and

$$f_\ell = F_\ell - F^s_\ell - \sum_{k=1}^{N}\sum_{i=1}^{E_k}(m^{ki}\dot{v}^{ki}_{qm}v^{ki}_{\ell m}y_q + I^{ki}_{mn}\dot{\omega}^{ki}_{qn}\omega^{ki}_{\ell m}y_q + e_{msp}\omega^{ki}_{qs}\omega^{ki}_{rn}\omega^{ki}_{\ell m}I^{ki}_{pn}y_q y_r) \tag{47}$$

The F_ℓ^s is given by Eq. (42), and F_ℓ is obtained from Eq. (40) as

$$F_\ell = \sum_{k=1}^{N} \sum_{i=1}^{E_k} (v_{\ell m}^{ki} F_m^{ki} + \omega_{\ell m}^{ki} M_m^{ki}) \tag{48}$$

Equations (45) and (11) can be numerically integrated by standard numerical integration algorithms to yield the time history of the generalized speeds and the generalized coordinates.

V. Simulations

A general purpose computer program for multibody systems has been developed utilizing the procedures presented in this paper. The program automatically eliminates the constrained joint degrees of freedom by deleting the corresponding rows in the partial velocity vectors, hence eliminating constraint equations for joint connections.

To show the significance of the geometric stiffening effects, the space-based robotic manipulator used by Kane et al.[20] will be considered (Fig. 3). Kane et al.[20] developed the equations of motion for a cantilever beam attached to a moving base and made use of the explicit constraint equation between the axial and transverse deflections in the derivation of the generalized inertia forces to obtain the related geometric stiffening terms.

Here, the same data for the manipulator in Fig. 3 will be used with the exception that the eccentricity components will be assumed to be zero; hence, their effects will not be considered. Links 1 and 2 are rigid, each with a length of 8 m. The flexible link contains two distinct segments, B_1 and B_2, with material properties $E = 6.895 \times 10^{10}$ N/m^2, $G = 2.6519 \times 10^{10}$ N/m^2, and mass density $\rho = 2766.67$ kg/m^3. The B_1 is $2\frac{2}{3}$ m long and has the following section properties: $A = 3.84 \times 10^{-4}$ m^2, $I_2 = 1.50 \times 10^{-7}$ m^4, $I_3 = 1.50 \times 10^{-7}$ m^4, $k_2 = 2.09$, $k_3 = 2.09$, and $\kappa = 2.2 \times 10^{-7}$ m^4. The B_2 is $5\frac{1}{3}$ m long and has the properties $A = 7.3 \times 10^{-5}$ m^2, $I_2 = 4.8746 \times 10^{-9}$ m^4, $I_3 = 8.2181 \times 10^{-9}$ m^4, $k_2 = 3.174$, $k_3 = 1.52$, and $\kappa = 2.433 \times 10^{-11}$ m^4.

First, the deployment maneuver lasting $T = 15$ s, during which the angles ψ_1, ψ_2, and ψ_3 change from 180 to 90 deg, 180 to 45 deg, and 180 to 0 deg, respectively, is simulated. The deployment motion is given as

$$\psi_1(t) = \begin{cases} \pi - \dfrac{\pi}{2T}\left(t - \dfrac{T}{2\pi}\sin\dfrac{2\pi t}{T}\right)\text{rad}, & 0 < t \leqslant T \\ \dfrac{\pi}{2}, & t > T \end{cases} \tag{49}$$

$$\psi_2(t) = \begin{cases} \pi - \dfrac{3\pi}{4T}\left(t - \dfrac{T}{2\pi}\sin\dfrac{2\pi t}{T}\right)\text{rad}, & 0 < t \leqslant T \\ \dfrac{\pi}{4}, & t > T \end{cases} \tag{50}$$

$$\psi_3(t) = \begin{cases} \pi - \dfrac{\pi}{T}\left(t - \dfrac{T}{2\pi}\sin\dfrac{2\pi t}{T}\right)\text{rad}, & 0 < t \leqslant T \\ 0, & t > T \end{cases} \tag{51}$$

The tip deflections u_2 and u_3 along $\mathbf{n}_2$ and $\mathbf{n}_3$, respectively, are given in Fig. 4. The displacement u_2 is identical to the simulation given in Ref. 20. Torsional deformations will not be reported, since the major part is due to the eccentricity, which also accounts for the small difference exhibited in Fig. 4b for the lateral deflection u_3, compared with the results of Ref. 20.

Second, the spin-up maneuver is simulated, for which the initial configuration is given by Fig. 5. The ψ_1 and ψ_3 are fixed at 90 and 0 deg, respectively, and $\dot{\psi}_2$ increases from 0 to 6 rad/s in a time interval of $T = 15$ s. This motion is given as

$$\psi_2(t) = \begin{cases} \dfrac{6}{T}\dfrac{t^2}{2} + \dfrac{T^2}{4\pi^2}\left(\cos\dfrac{2\pi t}{T} - 1\right) \text{ rad}, & 0 < t \leqslant T \\ (6t - 45) \text{ rad}, & t > T \end{cases} \tag{52}$$

Again, the tip transverse deflection is plotted in Fig. 6, and, as expected, identical results with Ref. 20 are obtained. This simulation shows clearly that without the proper stiffening expressions the simulations of spin-up motions may lead to completely incorrect results. Most importantly, this paper shows how the geometric nonlinearities can be accurately modeled in the strain energy function.

Spin-up motion together with deployment of other parts such as helicopter rotor blades and satellites with flexible appendages are of practical interest. For this reason, an additional simulation is performed. Starting from the initial

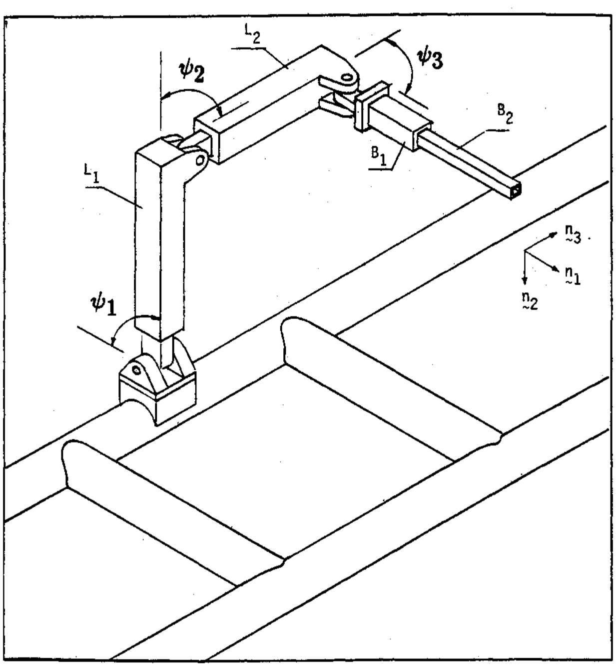

Fig. 3 Space-based manipulator.

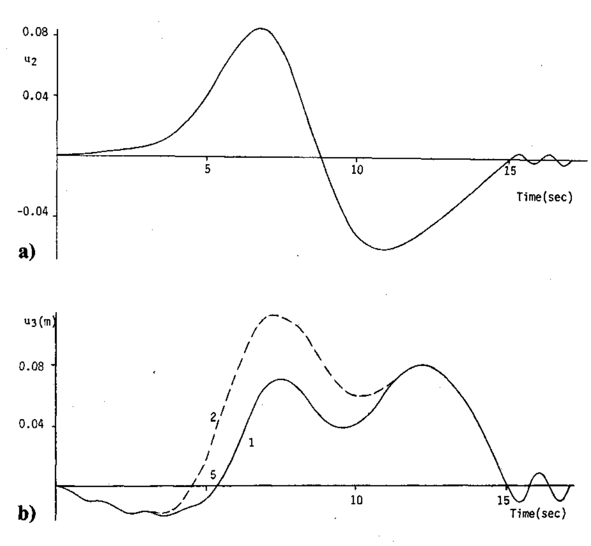

Fig. 4 Tip deflections: a) u_2; b) u_3. 1) Simulation of this paper. 2) Simulation by Kane et al.,[20] including eccentricity.

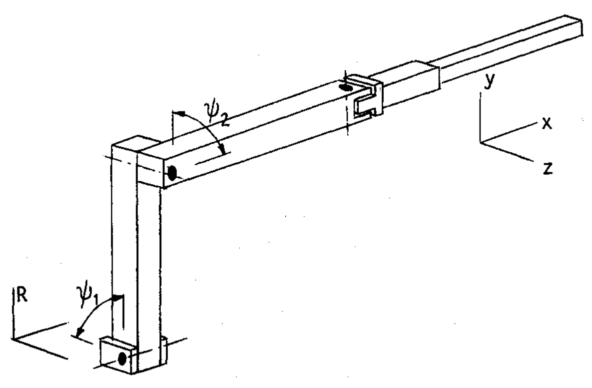

Fig. 5 Initial configuration for spin-up motion.

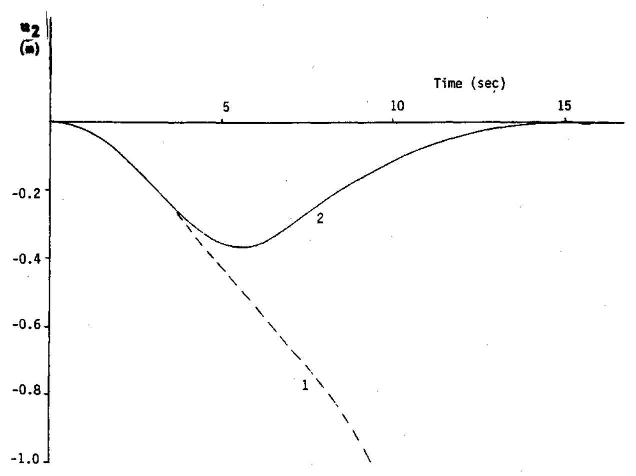

Fig. 6 Tip deflection, u_2 for spin-up motion: 1) without geometric stiffening; 2) with geometric stiffening.

configuration given in Fig. 5, in addition to the spin-up motion of link 2 given by Eq. (52), link 1 will be deployed from 90 to 40 deg as

$$\psi_1 = \begin{cases} \dfrac{\pi}{2} - \dfrac{5}{9}\dfrac{\pi}{2T}\left(t - \dfrac{T}{2\pi}\sin\dfrac{2\pi t}{T}\right)\text{rad}, & 0 < t \leqslant T \\ \dfrac{2\pi}{9}, & t > T \end{cases} \tag{53}$$

The tip deflections u_2 and u_3 for this simulation are given in Figs. 7 and 8. It can easily be seen that u_2 is affected by the additional centrifugal forces while following the same pattern. The deflection in the $\boldsymbol{n}^3$ direction, u_3 diverges when the geometric stiffening is not included. This is because centrifugal softening becomes the dominant effect stemming from high $\dot{\psi}_2$. Otherwise the u_3 deflection tends to stabilize with time when the geometric stiffening forces become dominant. The effect of the deployment acceleration on u_3 changes sign depending on ψ_2, which undergoes approximately seven revolutions in 15 s.

VI. Discussion and Conclusions

This paper presents a general procedure for the simulation and analysis of treelike multibody systems with rigid and flexible bodies. The nonlinear geometric stiffness matrix is developed for the general three-dimensional case where the effects of shear deformation are also included. The procedures developed show the complete interactions between the elastic deformations and gross rigid-body motion. Explicit expressions for the partial velocity and partial angular velocity vectors are given in a form suitable for computer implementation. The use of Kane's equations makes the analysis even more tractable once the partial velocities and partial angular velocities are fully developed.

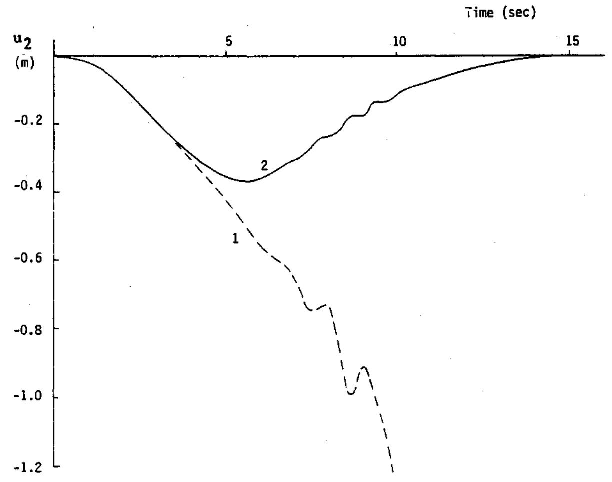

Fig. 7 Tip deflection, u_2 for spin-up and deployment motion: 1) without geometric stiffening; 2) with geometric stiffening.

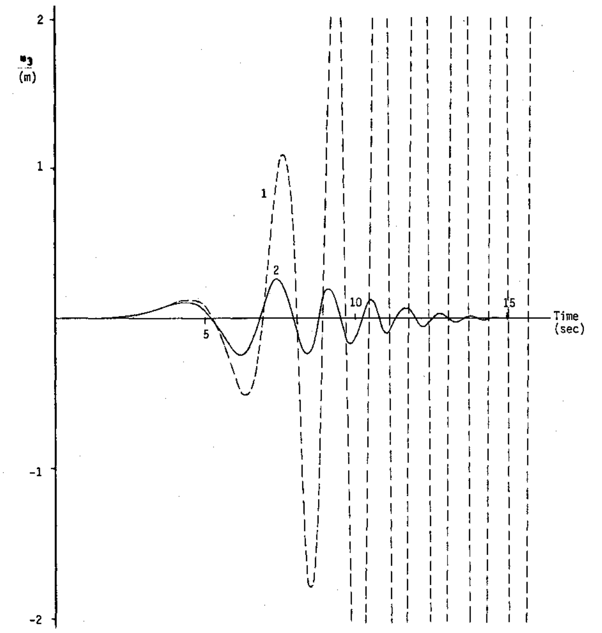

Fig. 8 Tip deflection, u_3 for spin-up and deployment motion: 1) without geometric stiffening; 2) with geometric stiffening.

The equations of motion in their developed form are also valid for other types of bodies if their corresponding shape function and stiffness matrices are used.

It is shown that geometric stiffening due to the coupling between the axial and transverse deformations has a dominant effect in high-speed spin-up and constant spin motions. In case the resulting axial forces are compressive, the coupling yields geometric softening of the transverse deformations. Failure to incorporate these effects leads to unreliable simulations.

Appendix A

Let the beam B_k be modeled by one-dimensional beam elements. Consider an element with nodes A and B. Let $u_p(x,t)$, $\theta_p(x,t)$ denote the elastic displacements and rotations of axis frames fixed along the centroid of the element.

The symbols u_p and θ_p are expressed in terms of the nodal variables e_j^{ki} by utilizing polynomials of appropriate order[24] as

$$u_p(x,t) = S_{pr} e_r^{ki}(t) \tag{A1}$$

and

$$\theta_p(x,t) = R_{pr} e_r^{ki}(t) \tag{A2}$$

where e_j^{ki} are the displacements and the rotations at the nodes

$$e^{ki} = [u_1^A, u_2^A, u_3^A, \theta_1^A, \theta_2^A, \theta_3^A, u_1^B, u_2^B, u_3^B, \theta_1^B, \theta_2^B, \theta_3^B]^T \tag{A3}$$

and the element shape functions S and R can be found in Refs. 24 and 27.

The eigenvalue problem can be expressed as[24]

$$M_{pj}^k \ddot{e}_j^k + K_{pj}^k e_j^k = 0 \tag{A4}$$

where M^k and K^k are the assembled mass and stiffness matrices after the application of the boundary conditions at the connection points, and e_j^k are the nodal coordinates of B_k. The approximate solution is

$$e_p^k = X_{pj}^k \eta_j^k; \qquad j = 1,\dots,M_k, \qquad p = 1,\dots,n^k \tag{A5}$$

where X^k is the matrix with eigenvectors as columns, η_j^k are the modal coordinates of B_k, and M_k is the number of eigenvectors used.

For simplicity of notation it will be assumed that the selected grid points are the finite-element mass centers. Then, using equation (A5), u_p^{ki} and θ_p^{ki} in Eqs. (1) and (2) can be expressed as

$$u_p^{ki} = S_{ps} B_{s\ell}^{ki} X_{\ell r}^k \eta_r^k = \phi_{pr}^{ki} \eta_r^k$$

$$p = 1,2,3, \quad s = 1,\dots,n^{ki}, \quad \ell = 1,\dots,n^k, \quad r = 1,\dots,M_k \tag{A6}$$

and

$$\theta_p^{ki} = R_{ps} B_{s\ell}^{ki} X_{\ell r}^k \eta_r^k = \psi_{pr}^{ki} \eta_r^k \tag{A7}$$

where the matrices S and R are evaluated at the mass center of the element. The B^{ki} is a Boolean matrix used for assembly, describing the indices of e^{ki} in e^k, such that

$$e_s^{ki} = B_{s\ell}^{ki} e_\ell^k \tag{A8}$$

Similarly, the local deformation displacement and rotation of $\boldsymbol{n}^{k*}$ with respect to $\boldsymbol{n}^j$, $j = \Gamma(k)$ can be expressed as

$$u_p^{k*} = S_{ps} B_{s\ell}^k X_{\ell r}^j \eta_r^j = \phi_{pr}^{k*} \eta_r^j \tag{A9}$$

and

$$\theta_p^{k*} = R_{ps} B_{s\ell}^{k*} X_{\ell r}^j \eta_r^j = \psi_{pr}^{k*} \eta_r^j \tag{A10}$$

where S and R are evaluated at the spatial coordinates of the corresponding element in B_j.

Appendix B

Using $u_p(x,t)$ and $\theta_p(x,t)$ as defined in Appendix A, the displacement field for arbitrary points in the beam element $v_p(x,y,z,t)$, $p = 1,2,3$ can be expressed, by assuming small rotations, as

$$v_1 = u_1 + z\theta_2 - y\theta_3 \tag{B1a}$$

$$v_2 = u_2 - z\theta_1 \tag{B1b}$$

$$v_3 = u_3 + y\theta_1 \tag{B1c}$$

where y and z are measured from the centroidal line.

Because of the presence of "large" deflections, the strain components ε_p, $p = 1,\dots, 6$ are obtained from nonlinear strain displacement relations using the displacements given by Eqs. (B1).

If the volume change of an infinitesimal element in the deformed body is negligible, the strain energy is given by[25]

$$\boldsymbol{u} = \frac{1}{2}\int_{v_{ki}} \boldsymbol{\varepsilon}^T \boldsymbol{\sigma}\, \mathrm{d}V \tag{B2}$$

where $\boldsymbol{\varepsilon}$ and $\boldsymbol{\sigma}$ are the vectors of strain and stress components, respectively. The $\boldsymbol{\varepsilon}_p$ are then substituted into Eq. (B2) to obtain $\boldsymbol{u}$, using the generalized Hook's law. The σ_2 and σ_3 can be taken to be zero. Fourth-order terms in $\partial u_2/\partial x$ and $\partial u_3/\partial x$, third-order terms in $\partial u_1/\partial x$ and $\partial \theta_p/\partial x$, $p = 1,2,3$, and second-order terms in $\partial \theta_p/\partial x$ multiplied by $\partial u_2/\partial x$ or $\partial u_3/\partial x$ are neglected. Furthermore, the shear deformation is assumed small so that third-order terms involving $(\partial u_2/\partial x) - \theta_3$ and $(\partial u_3/\partial x) + \theta_2$ are neglected. This yields the following additional terms in the strain energy:

$$U^G = \frac{EA}{2}\int \frac{\partial u_1}{\partial x}\left(\frac{\partial u_2}{\partial x}\right)^2 \mathrm{d}x + \frac{EA}{2}\int \frac{\partial u_1}{\partial x}\left(\frac{\partial u_3}{\partial x}\right)^2 \mathrm{d}x \tag{B3}$$

Assuming that the axial force $F = EA(\partial u_1/\partial x)$ is constant along the beam, and using Castigliano's theorem, the local geometrical stiffness matrix G^{ki} for the three-dimensional beam element is obtained as

$$G^{ki} = \frac{F}{L}\begin{bmatrix} 0 &&&&&&&&&&& \\ 0 & g_1 &&&&&&&& \text{symmetric} && \\ 0 & 0 & g_3 &&&&&&&&& \\ 0 & 0 & 0 & 0 &&&&&&&& \\ 0 & 0 & g_4 & 0 & g_5 &&&&&&& \\ 0 & g_2 & 0 & 0 & 0 & g_7 &&&&&& \\ 0 & 0 & 0 & 0 & 0 & 0 & 0 &&&&& \\ 0 & -g_1 & 0 & 0 & 0 & -g_2 & 0 & g_1 &&&& \\ 0 & 0 & -g_3 & 0 & -g_4 & 0 & 0 & 0 & g_3 &&& \\ 0 & 0 & 0 & 0 & 0 & 0 & 0 & 0 & 0 & 0 && \\ 0 & 0 & g_4 & 0 & g_6 & 0 & 0 & 0 & -g_4 & 0 & g_5 & \\ 0 & g_2 & 0 & 0 & 0 & g_8 & 0 & -g_2 & 0 & 0 & 0 & g_7 \end{bmatrix} \tag{B4}$$

where

$$g_1 = \frac{1}{(1+\lambda_2)^2}\left(\frac{6}{5} + 2\lambda_2 + \lambda_2^2\right) \tag{B5a}$$

$$g_2 = \frac{L}{10(1+\lambda_2)^2} \tag{B5b}$$

$$g_3 = \frac{1}{(1+\lambda_3)^2}\left(\frac{6}{5} = 2\lambda_3 + \lambda_3^2\right) \tag{B5c}$$

$$g_4 = \frac{-L}{10(1+\lambda_3)^2} \tag{B5d}$$

$$g_5 = \frac{L^2}{(1+\lambda_3)^2}\left(\frac{2}{15} + \frac{\lambda_3}{6} + \frac{\lambda_3^2}{12}\right) \tag{B5e}$$

$$g_6 = \frac{L^2}{(1+\lambda_3)^2}\left(-\frac{1}{30} - \frac{\lambda_2^2}{3}\right) \tag{B5f}$$

$$g_7 = \frac{L^2}{(1+\lambda_2)^2}\left(\frac{2}{15} + \frac{\lambda_2}{6} + \frac{\lambda_2^2}{12}\right) \tag{B5g}$$

$$g_8 = \frac{L^2}{(1+\lambda_2)^2}\left(-\frac{1}{30} - \frac{\lambda_2^2}{3}\right) \tag{B5h}$$

and

$$F = (EA/L)(u_1^B - u_1^A) \tag{B6}$$

In Eqs. (B5) λ_2 and λ_3 are given by

$$\lambda_2 = \frac{12EI_3}{k_2 GAL^2}, \qquad \lambda_3 = \frac{12EI_2}{k_3 GAL^2} \tag{B7}$$

where k_2 and k_3 are shear correction factors, A is the cross-sectional area, L is the length of the element, I_2 and I_3 are central principal second moments of area, E is the modulus of elasticity, and G is the shear modulus.

References

[1]Bodley, C. S., Devers, A. D., Park, A. C., and Frisch, H. P., "A Digital Computer Program for the Dynamic Interaction Simulation of Controls and Structure (DISCOS)," Vol. 1 and 2. NASA TP-1219, May 1978,

[2]Frisch, H. P., "A Vector-Dyadic Development of the Equations of Motion for N-Coupled Flexible Bodies and Point Masses," NASA TN D-8047, Aug. 1975.

[3]Ho, J. Y. L., "Direct Path Method for Flexible Multibody Spacecraft Dynamics," *Journal of Spacecraft and Rockets*, Vol. 14, Jan.–Feb. 1977, pp. 102–110.

[4]Ho, J. Y. L. and Herber, D. R., "Development of Dynamics and Control Simulation of Large Flexible Space Systems," *Journal of Guidance, Control, and Dynamics*, Vol. 8, May–June 1985, pp. 374–384.

[5]Singh, R. P., VanderVoort, R. J., and Likins, P. W., "Dynamics of Flexible Bodies in Tree Topology—A Computer Oriented Approach," AIAA Paper 84-1024, 1984.

[6]Huston, R. L., "Multibody Dynamics Including the Effects of Flexibility and Compliance," *Computer and Structures*, Vol. 14, No. 5–6, 1981, pp. 443–451.

[7]Singh, R. P. and Likins, P. W., "Manipulator Interactive Design with Interconnected Flexible Elements," *Proceedings of the American Control Conference*, American Automatic Control Council, IEEE Service Center, Paper TAG-11:00, 1983, pp. 505–512.

[8]Sunada, W. and Dubowsky, S., "The Application of Finite Element Methods to the Dynamic Analysis of Flexible Spatial and Co-Planar Linkage Systems," *ASME Journal of Mechanical Design*, Vol. 103, No. 3, July 1981, pp. 643–651.

[9]Book, W. J. and Majett, M., "Controller Design for Flexible Distributed Parameter Mechanical Arms Via Combined State Space and Frequency Domain Techniques," *ASME Journal of Mechanical Design*, Vol. 103, No. 3, July 1981, pp. 101–120.

[10]Bejczy, A. K. and Paul, R. P., "Simplified Robot Arm Dynamics for Control," *Proceedings of the 20th IEEE Conference on Decision and Control*, Inst. for Electrical and Electronics Engineers Control System Society, IEEE Service Center.

[11]Geradin, M., Robert, G., and Bernardin, C., "Dynamic Modelling of Manipulators with Flexible Members," *Advanced Software in Robotics*, edited by A. Danthine and M. Geradin, North-Holland, Amsterdam, 1983, pp. 27–42.

[12]Cannon, R. H. and Schmitz, E., "Initial Experiments on the End-Point Control of a Flexible One Link Robot," *International Journal of Robotics Research*, Vol. 3, No. 3, Fall 1984, pp. 62–75.

[13]Bodley, C. S. and Park, A. C., "The Influence of Structural Flexibility on the Dynamic Response of Spinning Spacecraft," AIAA Paper 72-348, 1972.

[14]Kulla, P., "Dynamics of Spinning Bodies Containing Elastic Rods," *Journal of Spacecraft and Rockets*, Vol. 9, April 1972, pp. 246–253.

[15]Hughes, P. C., "Dynamics of a Flexible Space Vehicle with Active Attitude Control," *Celestial Mechanics*, Vol. 9, Feb. 1974, pp. 21–39.

[16]Imam, I., Sandor, G. N., and Kramer, S. N. "Deflection and Stress Analysis in High Speed Planar Mechanisms with Elastic Links," *Journal of Engineering for Industry*, Vol. 95, May 1973, pp. 541–548.

[17]Yoo, W. S. and Haug, E. J., "Dynamics of Flexible Mechanical Systems Using Vibration and Static Correction Modes," *Journal of Mechanisms, Transmission and Automation in Design*, Vol. 108, No. 3, Sept. 1986, pp. 315–322.

[18]Turcic, D. A. and Midha, A., "Generalized Equations fo Motion for the Dynamic Analysis of Elastic Mechanism Systems," *Journal of Dynamic Systems, Measurement and Control*, Vol. 106, Dec. 1984, pp. 243–248.

[19]Gandhi, M. V. and Thompson, B. S., "The Finite Element Analysis of Flexible Components of Mechanical Systems Using a Mixed Variational Principle, ASME Paper 80-DET-64.

[20]Kane, T. R., Ryan, R. R., and Banerjee, A. K., "Dynamics of a Cantilever Beam Attached to a Moving Base," *Journal of Guidance, Control, and Dynamics*, Vol. 10, No. 2, March–April 1987.

[21]Kane, T. R. and Levinson, D. A., "Dynamics Theory and Applications," McGraw-Hill, New York, 1985.

[22]Huston, R. L. and Passarello, C., "Multibody Structural Dynamics Including Translation Between the Bodies," *Computers and Structures*, Vol. 11, 1980, pp. 715–720.

[23]Amirouche, F. M. L and Ider, S. K., "Determination of the Generalized Constraint Forces in Multibody Systems Dynamics Using Kane's Equations," *Journal of Theoretical and Applied Mechanics*, Vol. 7, No. 1, March 1988.

[24]Przemieniecki, J. S., *Theory of Matrix Structural Analysis*, McGraw-Hill, New York, 1968.

[25]Dym, C. L. and Shames, I. M., *Solid Mechanics, A Variational Approach*, McGraw-Hill, New York, 1973.

[26]Hurty, W. C., "Dynamic Analysis of Structural Systems Using Component Modes," *AIAA Journal*, Vol. 3, April 1965, pp. 678–685.

[27]Ider, S. K. and Amirouche, F. M. L., "A Recursive Formulation of the Equations of Motion for Articulated Structures with Closed-loops—An Automated Approach," *International Journal of Computers and Structures*, Vol. 30, No. 5, 1988.